2011

Simulation of electrospun nanofiber deposition on stationary and moving substrates

Linhua Liu
GE (China) Research and Development Center, Shanghai

Yuris A. Dzenis
University of Nebraska-Lincoln, ydzenis@unl.edu

Published in *Micro & Nano Letters* 6:6 (2011), pp. 408–411; doi: 10.1049/mnl.2011.0167

Submitted April 2, 2011; revised May 4, 2011.

Simulation of electrospun nanofiber deposition on stationary and moving substrates

Lihua Liu[1,2] and Yuris Dzenis[1]

1. Nanofiber Facility, Department of Engineering Mechanics, Nebraska Center for Materials and Nanoscience, University of Nebraska-Lincoln, Lincoln, NE 68588-0526, USA
2. GE (China) Research and Development Center, 1800 Cailun Road 2W010, Pudong, Shanghai 210203, People's Republic of China
Corresponding author — Y. Dzenis, email ydzenis@unl.edu

Abstract
Electrospinning produces continuous fibers with diameters from single nanometers to microns by jetting polymer solutions in high electric fields. Electrospun non-woven filamentary materials attract rapidly growing interest for broad range of applications. Properties of these materials depend on their nano- and microstructure that is determined in turn by the electric field and nanofiber collector. Despite critical importance, deposition of electrospun fibers on substrates has not yet been extensively studied theoretically and new methods of nanofiber collection continue to be developed mostly empirically. The objective of this Letter was to develop and demonstrate numerical simulation of electrospun nanofiber deposition on moving collectors. A dynamic model of nanofiber deposition onto a fast rotating drum was developed and used to simulate partial nanofiber alignment on this collector. The results were compared with the filamentary deposits in two classical stationary collection methods. Good agreement with experimental observations demonstrated predictive ability of simulations. The developed models can be used for the analysis of mechanisms of fiber deposition and alignment on substrates in various electric fields. Better understanding of dynamic nanofiber interaction with the electric field and collectors can lead to improved collector devices enabling one-step integrated nanomanufacturing of the designer nanofilamentary assemblies and architectures.

1. Introduction: Electrospinning is an emerging technology producing continuous nano- and microfibers by jetting polymer solutions in high electric fields. A thin polymer jet ejected from a liquid surface travels towards the oppositely charged electrode, gets elongated by the external and internal electric forces, experiences several types of instabilities and gets deposited on a collector in the form of non-woven mat of ultrafine fibers [1–5]. In the last 15 years, the process has been used to manufacture hundreds of synthetic and biological polymers into continuous fibers with diameters ranging from 1.5 nanometers to several microns. Continuous ceramic and carbon nanofilaments were produced by modified processes and co-axial electrospinning was applied for manufacturing hollow nanofibers.

Electrospun nanofibers have diameters from 1 to 4 orders of magnitude smaller than the diameters of conventional microfibers produced by mechanical drawing. As a result, electrospun nanofibers have very large surface area to mass ratios providing critical advantages to a variety of applications. Ultrafine fibers are also expected to have superior mechanical properties and several high-performance nanofibers are currently under development. Most importantly, unlike carbon nanotubes or other nanowires, nanorods and nanoparticles produced by the bottom-up synthetic growth methods, the top-down electrospinning process produces continuous nanofibers (i.e. infinite in length). This dual nano– macro nature enables easy and inexpensive handling and processing of electrospun nanofibers into applications. Integrated electromechanical controls can be used for integrated fabrication of nanofibrous assemblies. Last but not least, nanofiber continuity alleviates to a great extent the environmental and health concerns associated with discontinuous nanoparticles and nanotubes [3].

The interest in electrospinning and nanofibers is growing rapidly because of a large number of current and projected applications of electrospun nanofilamentary materials in filters, sensors, electronics, composites, energy conversion and storage devices, tissue engineering scaffolds, drug delivery carriers, wound dressings, implants, nanoprobes and many others [5–15]. Nanofiber material properties depend on their micro and nanoarchitecture. For example, elasticity of fiber networks depends on the filament diameters and orientation distributions [16, 17]. Many electrospun fiber applications can benefit from controlled nanofiber deposition and assembly. The final nanofilamentary architecture in electrospinning depends mostly on the electric field and nanofiber collector. Owing to massive jet instabilities, nanofibers collected on a generic continuous flat electrode usually exhibit random in-plane orientation. Many advanced nanofiber collection techniques have been developed over the years [18–24]. Some techniques resulted in high nanofiber alignment in small deposition areas [3, 20, 21]. However, perfect alignment over large deposition areas remains elusive. The most popular collection technique to date – nanofiber collection on a rotating drum [25, 26] – results in only partial nanofiber alignment that often further deteriorates with the increase of the deposition time because of the build-up of embedded residual charges in nanofiber deposits.

Poor deposition control may be in part owing to our lack of understanding of mechanisms of dynamic interactions of the fast-moving jets with the electric field and collectors. Currently, there are no models or simulations describing electrospun nanofiber deposition on moving substrates, such as the rotating drum. The goal of this Letter was to develop and demonstrate a simulation of such dynamic deposition. A model of nanofiber deposition onto a rotating drum was developed and used to simulate partial nanofiber alignment in this method. The results were compared with the filamentary constructs achieved on two classical stationary collectors. Numerical simulations were compared with experimental observations. The developed models can be used for the analysis of mechanisms of jet deposition and alignment on various collecting devices in arbitrary electric fields.

2. Dynamic jet motion and deposition simulation: A typical electrospinning process is depicted in Figure 1*a*. Polymer solution is stored in a syringe and forced through the syringe needle using a computerized micropump. At the beginning, a fluid drop or meniscus is formed at the end of the capillary needle. When critical voltage is reached, a jet of solution emerges from the meniscus and moves rapidly towards the collector. The charged jet is bent, stretched and twisted into complex shapes by the external and internal electric forces. This results in random nanofiber sheets deposited on the generic flat stationary nanofiber collector (Figure 1*a*).

Electrified jet can be discretized and represented by a series of particles with charge e and mass m connected by viscoelastic

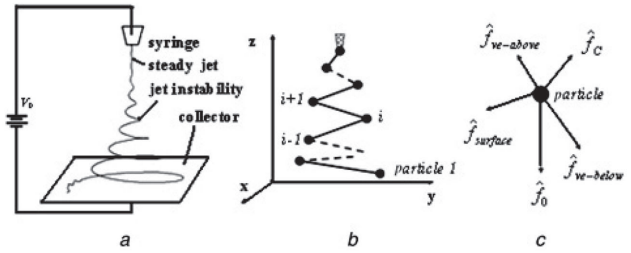

Figure 1. Schematic of electrospinning process (a) and numerical discretization of electrospun jets: electrified jet represented by a series of charged mass particles connected by viscoelastic elements (b) and forces acting on jet particles (c). $f_{\text{ve-above}}$ is the viscoelastic force from the particle above and $f_{\text{ve-below}}$ is the viscoelastic force from the particle below the current particle (i.e. up and down the jet). Gravity and frictional forces are neglected compared with the electrical and mechanical forces and surface tension.

elements (Figure 1*b*), by analogy with the model developed in [27]. The dynamic forces acting on jet particle (Figure 1*c*) can be defined as follows:

• *Electric force from the external field*

$$\hat{f}_0 = -e[\hat{i}E_x(t) + \hat{j}E_y(t) + \hat{k}E_z(t)] \tag{1}$$

where $E_x(t)$, $E_y(t)$ and $E_z(t)$ are the electric field components in x, y, and z directions, respectively; these components can be time varying, in general.

• *Coulomb force of particle-to-particle interaction*

$$\hat{f}_C = \sum_{\substack{j=1,N \\ j\neq i}} \frac{e^2}{R_{ij}^2}\left[\hat{i}\frac{x_i - x_j}{R_{ij}} + \hat{j}\frac{y_i - y_j}{R_{ij}} + \hat{k}\frac{z_i - z_j}{R_{ij}}\right] \tag{2}$$

where $\hat{i}$, $\hat{j}$, $\hat{k}$ are the unit vectors along the x, y, z axes, respectively; x_i, y_i, z_i, . . . are the Cartesian coordinates of the particle i, N is the total number of particles, and $R_{ij} = [(x_i - x_j)^2 + (y_i - y_j)^2 + (z_i - z_j)^2]^{1/2}$

• *Viscoelastic force*

$$\hat{f}_{ve} = \pi a_{ui}^2 \sigma_{ui}\left[\hat{i}\frac{x_{i+1} - x_i}{l_{ui}} + \hat{j}\frac{y_{i+1} - y_i}{l_{ui}} + \hat{k}\frac{z_{i+1} - z_i}{l_{ui}}\right] - \pi a_{di}^2 \sigma_{di}\left[\hat{i}\frac{x_i - x_{i-1}}{l_{di}} + \hat{j}\frac{y_i - y_{i-1}}{l_{di}} + \hat{k}\frac{z_i - z_{i-1}}{l_{di}}\right] \tag{3}$$

where a_{ui} and l_{ui} are, respectively, the radius and length of the connecting element between the ith and the $(i + 1)$th particles, a_{di} and l_{di} are, respectively, the radius and length of the connecting element between the ith and the $(i - 1)$th particles, which are given by

$$\pi a_{ui}^2 l_{ui} = \pi a_0^2 L, \quad \pi a_{di}^2 l_{di} = \pi a_0^2 L \tag{4}$$

where $L = (e^2/\pi a_0^2 G)^{1/2}$ is the initial length, a_0 is the initial jet cross-sectional radius at $t = 0$. σ_{ui}, σ_{fi} are the viscoelastic stresses that are defined by the viscoelastic Maxwellian fluid jet model [24] as

$$\frac{d\sigma_{ui}}{dt} = G\frac{1}{l_{ui}}\frac{dl_{ui}}{dt} - \frac{G}{\mu}\sigma_{ui}, \quad \frac{d\sigma_{di}}{dt} = G\frac{1}{l_{di}}\frac{dl_{di}}{dt} - \frac{G}{\mu}\sigma_{di} \tag{5}$$

where t is the time, G and μ are the elastic modulus and viscosity, respectively, and l is the filament length.

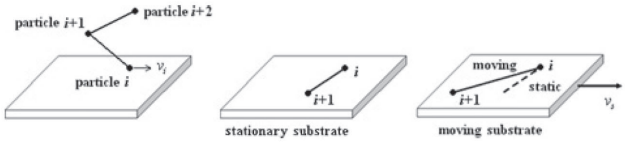

Figure 2. Schematic of jet deposition onto substrate: jet particle is assumed to stick to the collector once it hits the collector and particle velocity v_i becomes equal to the collector velocity.

• *Surface tension force*

$$\hat{f}_{\text{surface}} = -\frac{\alpha\pi(a^2)_{av}k_i}{(x_i^2 + y_i^2)^{1/2}}[\hat{i}|x_i|\text{sign}(x_i) + \hat{j}|y_i|\text{sign}(y_i)] \tag{6}$$

where α is the surface tension coefficient, k_i is the jet curvature, and

$$\begin{aligned} (a^2)_{av} &= (a_{ui} + a_{di})^2/4 \\ \text{sign}(x) &= 1, \quad \text{if } x > 0 \\ \text{sign}(x) &= -1, \quad \text{if } x < 0 \\ \text{sign}(x) &= 0, \quad \text{if } x = 0 \end{aligned} \tag{7}$$

Gravity and frictional forces from the air drag are neglected in comparison with the electrical and mechanical forces defined above.

The 3D dynamic equations of motion for the particle i are then written as follows

$$m\frac{d^2x_i}{dt^2} = \sum_{\substack{j=1,N \\ j\neq i}} \frac{e^2}{R_{ij}^2}\frac{x_i - x_j}{R_{ij}} + \frac{\pi a_{ui}^2\sigma_{ui}}{l_{ui}}(x_{i+1} - x_i) - \frac{\pi a_{di}^2\sigma_{di}}{l_{di}}(x_i - x_{i-1}) - \frac{\alpha\pi(a^2)_{av}k_i}{(x_i^2 + y_i^2)^{1/2}}[|x_i|\text{sign}(x_i)] - eE_x(t) \tag{8a}$$

$$m\frac{d^2y_i}{dt^2} = \sum_{\substack{j=1,N \\ j\neq i}} \frac{e^2}{R_{ij}^2}\frac{y_i - y_j}{R_{ij}} + \frac{\pi a_{ui}^2\sigma_{ui}}{l_{ui}}(y_{i+1} - y_i) - \frac{\pi a_{di}^2\sigma_{di}}{l_{di}}(y_i - y_{i-1}) - \frac{\alpha\pi(a^2)_{av}k_i}{(x_i^2 + y_i^2)^{1/2}}[|y_i|\text{sign}(y_i)] - eE_y(t) \tag{8b}$$

$$m\frac{d^2z_i}{dt^2} = \sum_{\substack{j=1,N \\ j\neq i}} \frac{e^2}{R_{ij}^2}\frac{z_i - z_j}{R_{ij}} + \frac{\pi a_{ui}^2\sigma_{ui}}{l_{ui}}(z_{i+1} - z_i) - \frac{\pi a_{di}^2\sigma_{di}}{l_{di}}(z_i - z_{i-1}) - eE_z(t) \tag{8c}$$

Note that unlike [27], all three components of the electric field are taken into account in the dynamic equations (8). These components are computed for the actual 3D field distribution, which may be static or dynamic, for example, oscillating or changing in other variable fashion.

Nanofiber deposition simulation: The dynamic jet motion model was augmented with the deposition simulation. The simulation of nanofiber deposition onto collectors is illustrated in Figure 2. For a stationary collector, it was assumed that once the jet particle hits the collector its velocity *vi* becomes zero. For a moving collector, the particle velocity is assumed to be equal the substrate velocity v_s, meaning that possible skidding of the particles with respect to the collector is neglected. Without loss of generality, for the purpose of the comparative demonstration of the effects of field configuration and collector motion, the charges of all deposited particles were assumed to vanish that implied good conduction of the collectors and reasonable charge motility in the deposited nanofi-

bers. This restriction can be removed in further studies, for example to simulate the effects of the residual charge build-up on alignment. The interaction of the deposited nanofiber with the moving substrate and the effect of substrate motion on nanofiber orientation is illustrated in Figure 2. The jet segment is stretched and partially aligned along the direction of motion of the substrate.

3. Numerical examples: The above modeling framework was applied to simulate dynamic nanofiber deposition in three popular electrospinning configurations (Figure 3). Figure 3*a* shows the generic electrospinning process with a traditional flat continuous collector. Deposition onto a rotating drum as a collector is illustrated in Figure 3*b*. Figure 3*c* shows an alignment method utilizing split electrodes, a technique often referred to as the 'gap' method.

In the simulations, the voltage V_0 was 12 kV; the distance between the tip of the syringe and the collector h was 40 cm (for the drum collector, this distance was from the tip to the top of the drum). The properties of aqueous polyethyleneoxide (PEO) electrospun polymer jets [27] were used in the simulations: the initial diameter of the jet a_0 was 150 μm, density ρ was 103 kg/m^3, α is 0.7 kg/s^2, μ was 10^3 kg/(m s), relaxation time θ was 10 ms, $G = \theta \cdot \mu$. For the rotating drum configuration, the diameter and length of the drum were 16 and 28 cm, respectively. The rotation speed was 800 rpm. The simulation parameters for the "gap" alignment method were as follows: the gap length was 12 cm; the dimensions of the two electrodes were 6 by 10 cm. During the simulations, initial small random perturbation displacement was applied to each newly generated particle ejected from the tip of the syringe. Random perturbations were deemed more realistic than the rotational perturbation adopted in [27]. Through dynamic simulations, patterns of the deposited nanofibers were obtained. Representative sections of the resulting nanofiber deposits from the middle of the deposition area in each of the three simulated cases are shown in Figure 4. Owing to the instabilities of the electrified jet, the deposition orientation of electrospun fibers on the traditional flat collector was random. Using rotating drum as collector, partially oriented nanofibers were predicted. Higher orientation of nanofibers was predicted for the "gap" alignment method.

4. Experimental observations: The three electrospinning setups in Figure 3 were implemented experimentally. PEO solution (4.5% wt) was delivered through a syringe with the inner diameter 1 mm. A voltage of 12 kV was applied between the syringe and the collector by a HP E3611A DC power supply connected with a Gamma HV power converter UC5-30P. The distance between the syringe and collector was 40 cm. The diameter and length of the drum were 16 and 28 cm, respectively. The rotation speed was 800 rpm. The gap size was 12 cm. The dimensions of the split electrodes in the gap method were 6 by 10 cm. When the applied voltage between the syringe and the collector exceeded a certain threshold, the electric forces in the liquid meniscus overcame the surface tension forces, which resulted in the formation of a fine polymer jet. Owing to instabilities, the jet experienced multiple bends and expanding loops before getting finally deposited onto substrates.

The deposited nanofibers were investigated using scanning electron microscopy (SEM). The results are presented in Figure 5. Experimental results showed that random electrospun fibrous sheets were obtained on the traditional stationary collector (Figure 5*a*). Partially oriented fibrous sheets were obtained by using the rotating drum as the collector (Figure 5*b*). Higher nanofiber alignment was observed across the gap in the split electrode or gap method (Figure 5*c*). Experimental results show good agreement with the simulated deposition patterns for all three fiber collection methods.

5. Conclusions: A model of nanofiber deposition onto a fast rotating drum was developed for the first time and used to simulate partial nanofiber alignment on that collector. The results were compared with the simulated nanofiber deposits in the stationary generic and gap methods. All three simulated predictions correlated well with the experimental observations. Note that, as shown in Figure 2, the proposed simulation not only describes the nanofiber alignment on a rotating drum, but also captures additional stretch because of the pull exerted on the deposited nanofiber by the moving drum surface. The latter has been shown important for some nanofibers such as piezoelectric polymer nanofibers [26]. This effect can be further optimized with the help of the developed dynamic deposition simulation. The demonstrated modeling framework can be applied for arbitrary-shaped stationary or moving collectors and various static or dynamic (e.g. oscillating) 3D field configurations. Advanced collecting methods such as the ones described in [28–31] can be modeled and further optimized. The demonstrated simulations can be used to study the mechanisms of jet interactions with collectors and alignment on various substrates that can lead to improved collection devices enabling single-step controlled dynamic deposition of designer nanofilamentary assemblies and constructs.

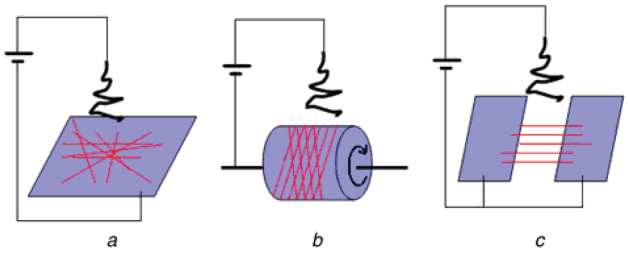

Figure 3. Schematic of the three popular nanofiber collection set-ups.
a. Traditional collector
b. Rotating drum
c. Gap method

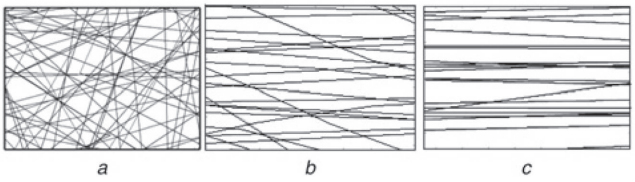

Figure 4. Simulated deposits of electrospun fibers for the three collection methods.
a. Traditional collector
b. Rotating drum
c. Gap method

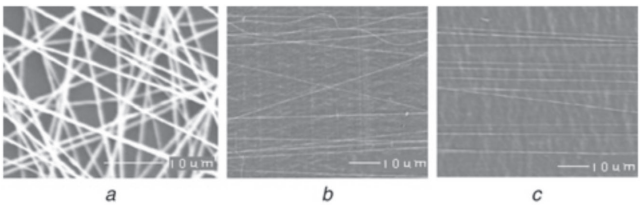

Figure 5. SEM images of nanofiber deposits for three different collection methods.
a. Traditional collector
b. Rotating drum
c. Gap method

6. Acknowledgments: This research was supported in part by the grants from the National Science Foundation, Army Research Office and Nebraska Research Initiative. L. Liu is grateful for the support from the graduate Othmer Fellowship, College of Engineering, University of Nebraska–Lincoln.

7 References

[1] Reneker D.H., Chun I.: "Nanometre diameter fibres of polymer, produced by electrospinning," *Nanotechnology*, 1996, **7**, pp. 216–223

[2] Li D., Xia Y.N.: "Electrospinning of nanofibers: Reinventing the wheel?," *Adv. Mater.*, 2004, **16**, (14), pp. 1151–1170

[3] Dzenis Y.: "Spinning continuous fibers for nanotechnology," *Science*, 2004, **304**, (5679), pp. 1917–1919

[4] Greiner A., Wendorff J.H.: "Electrospinning: A fascinating method for the preparation of ultrathin fibres," *Angew. Chem. Int. Ed.*, 2007, **46**, (30), pp. 5670–5703

[5] Filatov Y., Budyka A., Kirichenko V.: "Electrospinning of micro- and nanofibers: Fundamentals and applications in separation and filtration processes" (Begell House Inc., New York, USA, 2007)

[6] Ding B., Wang M., Wang X., *et al.*: "Electrospun nanomaterials for ultrasensitive sensors," *Mater. Today*, 2010, **13**, (11), pp. 16–27

[7] Lu X.F., Wang C., Wei Y.: "One-dimensional composite nanomaterials: Synthesis by electrospinning and their applications," *Small*, 2009, **5**, (21), pp. 2349–2370

[8] Chew S.Y., Wen Y., Dzenis Y., *et al.*: "The role of electrospinning in the emerging field of nanomedicine," *Curr. Pharm. Des.*, 2006, **12**, (36), pp. 4751–4770

[9] Dzenis Y.: "Structural nanocomposites," *Science*, 2008, **319**, (5862), pp. 419–420

[10] Agarwal S., Greiner A., Wendorff J.H.: "Electrospinning of manmade and biopolymer nanofibers-progress in techniques, materials, and applications," *Adv. Funct. Mater.*, 2009, **19**, (18), pp. 2863–2879

[11] Kriegel C., Arrechi A., Kit K., *et al.*: "Fabrication, functionalization, and application of electrospun biopolymer nanofibers," *Crit. Rev. Food Sci. Nutr.*, 2008, **48**, (8), pp. 775–797

[12] Liang D., Hsiao B.S., Chu B.: "Functional electrospun nanofibrous scaffolds for biomedical applications," *Adv. Drug Deliv. Rev.*, 2007, **59**, (14), pp. 1392–1412

[13] Schiffman J.D., Schauer C.L.: "A review: Electrospinning of biopolymer nanofibers and their applications," *Polymer Rev.*, 2008, **48**, (2), pp. 317–352

[14] Smith L.A., Liu X.H., Ma P.X.: "Tissue engineering with nanofibrous scaffolds," *Soft Matter*, 2008, **4**, (11), pp. 2144–2149

[15] Yoo H.S., Kim T.G., Park T.G.: "Surface-functionalized electrospun nanofibers for tissue engineering and drug delivery," *Adv. Drug Deliv. Rev.*, 2009, **61**, (12), pp. 1033–1042

[16] Wu X.F., Dzenis Y.A.: "Elasticity of planar fiber networks," *J. Appl. Phys.*, 2005, **98**, (9), pp. 093501–093509

[17] Thomas V., Jose M.V., Chowdhury S., *et al.*: "Mechanomorphological studies of aligned nanofibrous scaffolds of polycaprolactone fabricated by electrospinning," *J. Biomater. Sci.-Polym. Ed.*, 2006, **17**, (9), pp. 969–984

[18] Deitzel J.M., Kleinmeyer J.D., Hirvonen J.K., Beck Tan N.C.: "Controlled deposition of electrospun poly (ethylene oxide) fibers," *Polymer*, 2001, **42**, (19), pp. 8163–8170

[19] Ramakrishna S., Fujihara K., Teo W.-E., Lim T.-C., Ma Z.: "An introduction to electrospinning and nanofibers" (World Scientific Publishing, 2005, vol. 382)

[20] Theron A., Zussman E., Yarin A.L.: "Electrostatic fieldassisted alignment of electrospun nanofibres," *Nanotechnology*, 2001, **12**, (3), pp. 384–390

[21] Li D., Wang Y.L., Xia Y.N.: "Electrospinning of polymeric and ceramic nanofibers as uniaxially aligned arrays," *Nano Lett.*, 2003, **3**, (8), pp. 1167–1171

[22] Sundaray B., Subramanian V., Natarjan T.S.: "Electrospinning of continuous aligned polymer fibers," *Appl. Phys. Lett.*, 2004, **84**, (7), pp. 1222–1224

[23] Teo W.E., Ramakrishna S.: "Electrospun fibre bundle made of aligned nanofibres over two fixed points," *Nanotechnology*, 2005, **16**, (9), pp. 1878–1884

[24] Kim G.H., KimW.D.: "Formation of oriented nanofibers using electrospinning," *Appl. Phys. Lett.*, 2006, **88**, (23), pp. 233101–233103

[25] Barhate R.S., Loong C.K., Ramakrishna S.: "Preparation and characterization of nanofibrous filtering media," *J. Membr. Sci.*, 2006, **283**, (1–2), pp. 209–218

[26] Nasir M., Kotaki M.: "Fabrication of aligned piezoelectric nanofibers by electrospinning," *Int. J. Nanosci.*, 2009, **8**, (3), pp. 231–235

[27] Reneker D.H., Yarin A.L., Fong H., Koombhongse S.: "Bending instability of electrically charged liquid jets of polymer solutions in electrospinning," *J. Appl. Phys.*, 2000, **87**, (9), pp. 4531–4547

[28] Katta P., Alessandro M., Ramsier R.D., Chase G.G.: "Continuous electrospinning of aligned polymer nanofibers onto a wire drum collector," *Nano Lett.*, 2004, **4**, (11), pp. 2215–2218

[29] Li D., Ouyang G., McCann J.T., Xia Y.: "Collecting electrospun nanofibers with patterned electrodes," *Nano Lett.*, 2005, **5**, (5), pp. 913–916

[30] Yang Y., Jia Z., Hou L., *et al.*: "Controlled deposition of electrospinning jet by electric field distribution from an insulating material surrounding the barrel of the polymer solution," *IEEE Trans. Dielectr. Electr. Insul.*, 2008, **15**, (1), pp. 269–276

[31] Zucchelli A., Fabiani D., Gualandi C., Focarete M.L.: "An innovative and versatile approach to design highly porous, patterned, nanofibrous polymeric materials," *J. Mater. Sci.*, 2009, **44**, (18), pp. 4969–4975